Nuclear Engineering and Design 326 (2018) 268–284

Contents lists available at ScienceDirect

Nuclear Engineering and Design

journal homepage: www.elsevier.com/locate/nucengdes

Using seismic isolation to reduce risk and capital cost of safety-related nuclear structures

Ching-Ching Yu[a,*], Chandrakanth Bolisetti[b], Justin L. Coleman[b], Ben Kosbab[c], Andrew S. Whittaker[a]

[a] University at Buffalo, The State University of New York, 212 Ketter Hall, Amherst, NY 14260, USA
[b] Idaho National Laboratory, 2525 Fremont Avenue, Idaho Falls, ID 83402, USA
[c] SC Solutions, 188 Anderson St SE, Suite 250, Marietta, GA 30060, USA

ARTICLE INFO

Keywords:
Nuclear facilities
Seismic isolation
Seismic probabilistic risk assessment
Capital cost

ABSTRACT

The implementation of seismic base isolation can substantially reduce horizontal seismic demands on structures, systems, and components (SSCs) in a nuclear facility, potentially providing significant benefits in terms of increased safety (smaller seismic risk) and reduced capital construction cost. Although increased safety of SSCs has been demonstrated previously, the possible reduction in their capital cost has not been explored. To quantify the reduction in risk enabled by isolation, nonlinear response-history analysis of a conventionally founded and a base-isolated model of a generic nuclear facility (GNF) is performed at the sites of the Idaho National Laboratory and the Los Alamos National Laboratory: sites of moderate and high seismic hazard, respectively. Seismic probabilistic risk assessment is performed to compute the mean annual frequency of unacceptable performance. The seismic risk is reduced by 7 to 8 orders of magnitude by the implementation of isolation. The costs of addressing seismic loadings are estimated for the GNF in both the conventionally founded and base-isolated GNF. The possible reductions in the required seismic ruggedness and in the cost of SSCs in the isolated GNF are quantified at both sites. A reduction in cost enabled by isolation is possible at nearly all sites of nuclear facilities in the United States, with the greatest benefit at sites of high seismic hazard, such as LANL. Two risk-calculation procedures are used in the assessment: a simplified method based on Boolean mathematics and a rigorous method based on Monte Carlo analysis. The simplified procedure, which is suitable for implementation with preliminary design calculations, produces accurate estimates of risk unless the mean annual frequencies of unacceptable performance are very small, measured here as smaller than 10^{-10}. The sensitivity of the calculated risk in the conventionally founded GNF, to the choice of anchor period for the seismic hazard curve, is investigated and found to be insignificant over the range considered: 0 to 0.10 s.

1. Introduction

The reduction in horizontal seismic demands enabled by the use of seismic isolation yields four possible benefits for nuclear facilities: 1) economic: reduction in capital cost, 2) increased safety: reduction in the mean annual frequency of unacceptable performance, 3) insurance: protection against increases in the known seismic hazard during and after construction by minimizing or eliminating the effort to re-qualify and re-certify, or back-fit structures, systems and components, and 4) recertification: the opportunity to certify an existing NPP design for a region of higher seismic hazard. To date, only the second benefit has been explored (e.g., Huang et al., 2008a, 2011a, 2011b). In this paper, the potential benefits of reduced capital cost and increased safety are investigated for an archetype building, described herein as a generic nuclear facility (GNF).

To enable some generalization of the outcomes, two sites are considered for a conventionally founded and a base-isolated GNF: 1) the Idaho National Laboratory (INL) in Idaho Falls, ID and 2) the Los Alamos National Laboratory (LANL) in Los Alamos, NM. Seismic hazard calculations are performed and suites of ground motion time series are generated for each site. The GNF is assumed to handle materials at risk (MAR) and so structures, systems and components (SSCs) that are common to safety-related nuclear structures are used to populate the facility for risk calculations. The finite element code LS-DYNA (LSTC, 2013) is used to perform nonlinear response-history analysis of the conventionally founded (non-isolated) and base-isolated building; the

* Corresponding author.
E-mail address: cyu23@buffalo.edu (C.-C. Yu).

https://doi.org/10.1016/j.nucengdes.2017.11.016
Received 15 March 2017; Received in revised form 27 October 2017; Accepted 4 November 2017

isolated building is assumed to have a translational period of 2 s, and the isolation system was not optimized for either minimum risk or minimum cost. Horizontal seismic demands on the assumed SSCs are generated to enable risk and capital cost calculations. The seismic probabilistic risk assessment methodology as proposed by Huang et al. (2008a, 2011a,b) is used because it can accommodate highly nonlinear soils, isolators and structures. Two procedures are used for the calculations: 1) the rigorous Monte Carlo-based documented in Huang et al. (2008a, 2011a,b) and identified in ASCE/SEI Standard 4-16 (ASCE, 2017), and 2) a simplified method based on Boolean mathematics and basic probability theory. Only the effects of horizontal shaking are considered in this paper because available representative fragility data for the assumed SSCs less rigorously account for the effects of vertical earthquake shaking. The nuclear facility cost data proposed by Stevenson (1981, 2003), which estimates the cost contribution due to seismic considerations, are used to estimate 1) overnight capital cost (OCC) and 2) cost of SSCs for the conventionally founded and base-isolated building at both sites because no more modern, peer-reviewed data are available.

2. Description of the facility

2.1. Building framing and SSCs

The GNF is a two-story reinforced concrete building. The building is surface founded on a 5-ft. thick basemat. The thickness of the reinforced concrete walls ranges between 1 ft. and 3 ft. The building's plan dimensions are 65 ft. × 160 ft. At its highest point, the building is approximately 38 ft. tall. The total weight of the building, including the basemat, but excluding SSCs, is 21,280 kips.

This nuclear facility is assumed to handle materials at risk (MAR) and so sample SSCs in safety-related nuclear structures are used to populate the building. The SSCs are chosen from the Electric Power Research Institute (EPRI) Seismic probabilistic risk assessment implementation guide EPRI (2013), and include 1) motor control center (MCC), 2) battery, 3) coolant pump, 4) air handler, 5) heating, ventilation, air conditioning (HVAC) duct, 6) structure (surrounds the pressure vessel), 7) pressure vessel, and 8) piping. (The numbers are used later to identify the SSCs in the fault tree.)

2.2. Numerical modeling of the building

The finite element code LS-DYNA is used to model the GNF and perform response-history analysis. Two models are prepared: conventionally founded and base-isolated. Soil-structure-interaction (SSI) analysis is not performed for either model because generic soil conditions are assumed, as described in Section 3. Fig. 1a presents the LS-DYNA model of the conventionally founded GNF, identifying the global coordinate system (X, Y, Z) and representative dimensions. Fig. 1b through Fig. 1f present the finite element models of the basemat, walls, slabs and roofs. The elements were assigned linear elastic material properties consistent with concrete: Young's modulus, E, of 5.2×10^5 kip/ft^3, Poisson's ratio, ν, of 0.17, and mass density of 4.7×10^{-3} kip-s^2/ft^4. The total live load is 3115 kips, resulting from an assumed uniformly distributed load of 200 lb/ft^2 on the slabs and basemat, and of 100 lb/ft^2 on the roofs. The seismic (reactive) weight is taken as the dead load and one half of the live load (= 22,845 kips) per ASCE/SEI 7-10 (ASCE, 2010). Further details of the model can be found in Bolisetti et al. (2016).

The building responds dynamically in many modes. More than 900 modes are required to capture 90% of the total mass in the X, Y and Z directions (see Fig. 1). Table 1 presents summary information on the modal properties of the LS-DYNA model, including the seven modes that contribute most significantly to the modal effective mass (MEM) in each orthogonal direction. Modes are listed in a descending order of their contribution to MEM, rounded to the nearest percent. In the X direction, modes 5, 6, 9, 7, 12, 16, and 4 contribute 72% of the mass; in the Y direction, modes 4, 3, 5, 11, 7, 20, and 1 contribute 76% of the mass; and in the Z direction, modes 40, 18, 93, 26, 38, 29, and 43 contribute 38% of the mass. The GNF is stiffer than many of the commercial large light water reactors in the US fleet.

3. Seismic hazard calculations and ground motion time series generations

To ensure that the conclusions drawn from the study were applicable to a wide range of new-build nuclear facilities in the United States, isolation systems, risk calculations and cost estimates were prepared for two sites: 1) the Idaho National Laboratory (INL) in Idaho Falls, ID, assumed to represent low-to-moderate seismic hazard, and 2) the Los Alamos National Laboratory (LANL) in Los Alamos, NM, which represents a site of high seismic hazard. Seismic hazard data for INL and LANL were developed using the ground motion calculator at the website of the United States Geological Survey (USGS https://geohazards.usgs.gov/hazardtool/application.php, accessed on June 1, 2016). The soil condition at the INL and LANL sites of the GNF is assumed to be at the boundary between site classes B and C per ASCE/SEI Standard 7-10 (ASCE, 2010) for the seismic hazard calculations. Fig. 2a (Fig. 2b) presents seismic hazard curves at periods of 0.10 s (representative of a stiff nuclear facility) and 2 s (representative of the isolated GNF) at INL (LANL). (Hazard curves for the LANL and INL sites at periods between 0.0 and 0.10 s are not provided at the USGS website. The effect of the choice of anchor period for the seismic hazard curve is investigated later in the paper, in Appendix A.) Uniform hazard acceleration response spectra corresponding to a mean annual frequency of exceedance (MAFE) of 10^{-4} for the two sites are generated for horizontal shaking, and these are used to represent design basis earthquake (DBE) shaking. The design basis earthquake (DBE) horizontal acceleration spectra for 5% damping ratio are presented in Fig. 3 in linear and logarithmic scales.

Ground motion time series are generated to be compatible with the geometric mean spectra of Fig. 3. The seed motions are recorded ground motions. Thirty sets of two-horizontal-component ground motions are generated for the two sites in three steps:

(1) Select seed motions based on the 2-s peak magnitude-distance (M, r) pairs from the deaggregation tool provided at the USGS website (http://geohazards.usgs.gov/deaggint/2008/, accessed on June 1, 2016) for the sites:
   - INL, ID, 2 s: 6.8, 14.6 km (9.1 miles)
   - LANL, NM, 2 s: 6.8, 4.8 km (3.0 miles)

   The seed motions are extracted from the Pacific Earthquake Engineering Research (PEER) Center Ground Motion Database website (http://ngawest2.berkeley.edu/, accessed on June 1, 2016).

(2) Match the seed motions to the target spectrum using a time-domain procedure of RSPMatch2005 (Hancock et al., 2006). The matched acceleration spectra for 5% damping at the INL (LANL) site are presented in Fig. 4a and b (Fig. 5a and b).

(3) Scale the amplitudes of the two horizontal components in each set by factors to provide maximum direction-minimum direction (max-min) ground motions that recover the geometric mean (Huang et al., 2008b, 2009a,b). Amplitude scale factors F_h and $1/F_h$ are applied to the two horizontal components in each set, and were selected by a Latin Hypercube procedure from a lognormal distribution with a mean, θ, of 1.3 and a logarithmic standard deviation, β, of 0.13 (see Huang et al. (2008b) for details). The max-min ground motion acceleration spectra for 5% damping at the INL (LANL) site are presented in Fig. 4c and d (Fig. 5c and d).

Fig. 1. LS-DYNA model of the GNF.

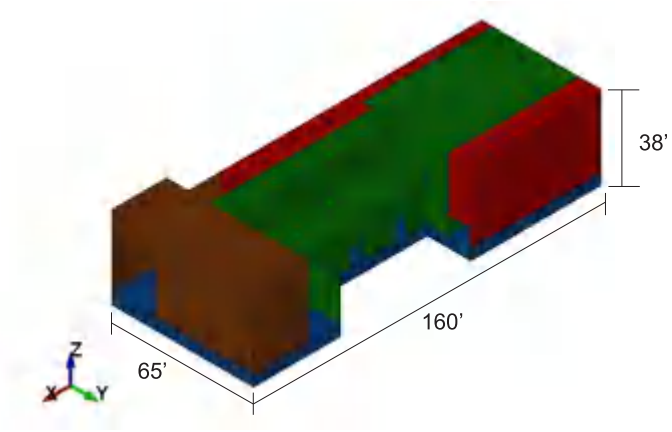

a. schematic view

b. basemat (solid elements)

c. walls (shell elements)

d. cell walls and roof (shell elements)

e. corridor walls, slab and roof (shell elements)

f. transfer corridor walls and roof (shell elements)

Table 1
Modal properties of the LS-DYNA model, ordered by modal effective mass.[1]

X direction			Y direction			Z direction		
Mode	Period (sec)	MEM (%)	Mode	Period (sec)	MEM (%)	Mode	Period (sec)	MEM (%)
5	0.047	24	4	0.050	40	40	0.021	11
6	0.042	14	3	0.051	19	18	0.028	6
9	0.037	10	5	0.047	8	93	0.015	5
7	0.042	7	11	0.036	4	26	0.024	5
12	0.035	6	7	0.042	2	38	0.021	4
16	0.030	6	20	0.026	2	29	0.024	4
4	0.050	5	1	0.099	2	43	0.020	3

[1] MEM rounded to the nearest 1%.

The orientation of the maximum-direction shaking was assigned randomly, with 15 of the 30 ground motions aligning with the global X direction (see Fig. 1) and the remaining 15 aligning with the global Y direction. These pairs of motions are used for response-history analysis.

4. Design and modeling of the isolation system

Three types of seismic isolators are identified in Chapter 12 of ASCE/SEI Standard 4-16 as pre-qualified for use in nuclear facilities in the United States: 1) low damping rubber, 2) lead rubber (LR), and 3) Friction Pendulum™ (FP). An isolation system composed of many LR bearings is assumed here but near identical results would be seen if FP bearings had been adopted. The LR bearing assumed for this study is circular and composed of alternating layers of low damping natural rubber and steel shim plates. A central, cylindrical lead plug dissipates

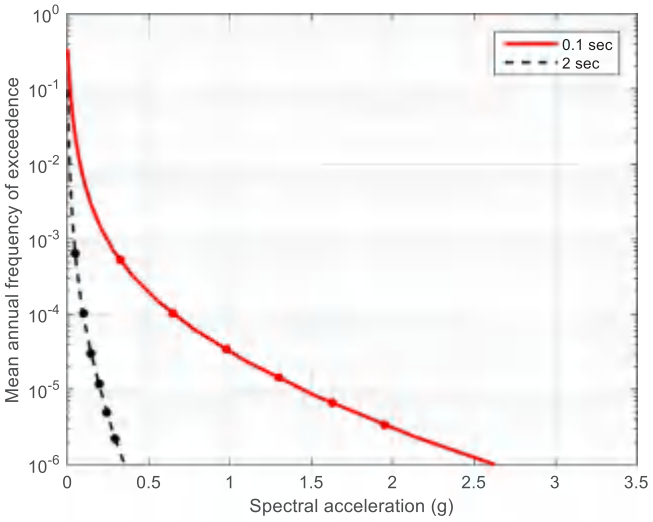

a. INL

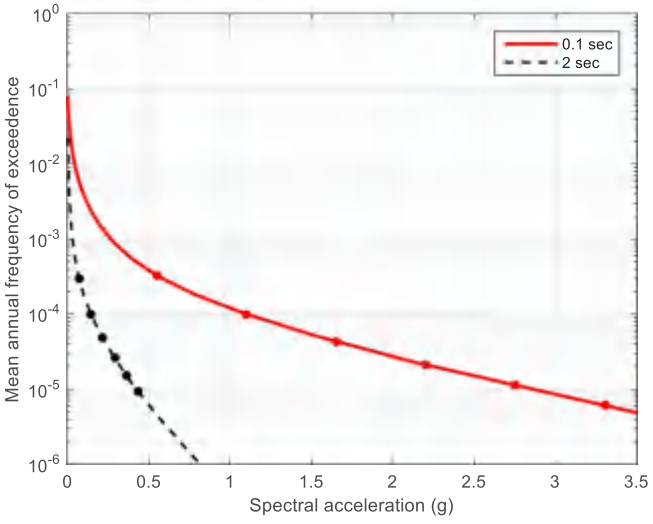

b. LANL

Fig. 2. Seismic hazard curves for 5% damping at 0.1 s and 2.0 s at INL and LANL.

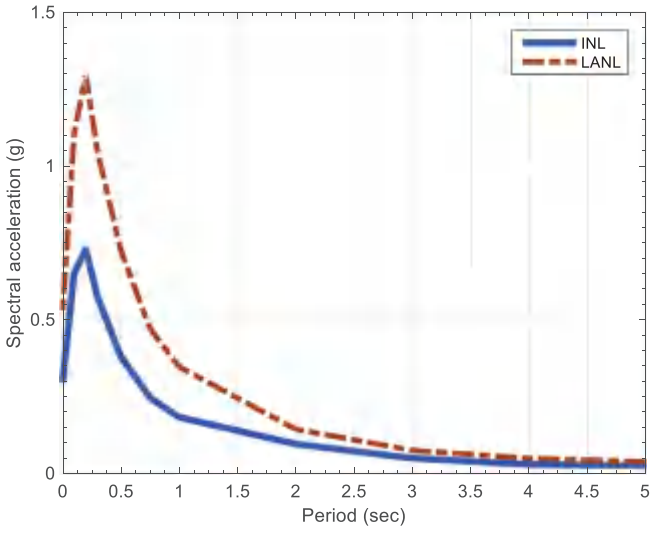

a. linear scale

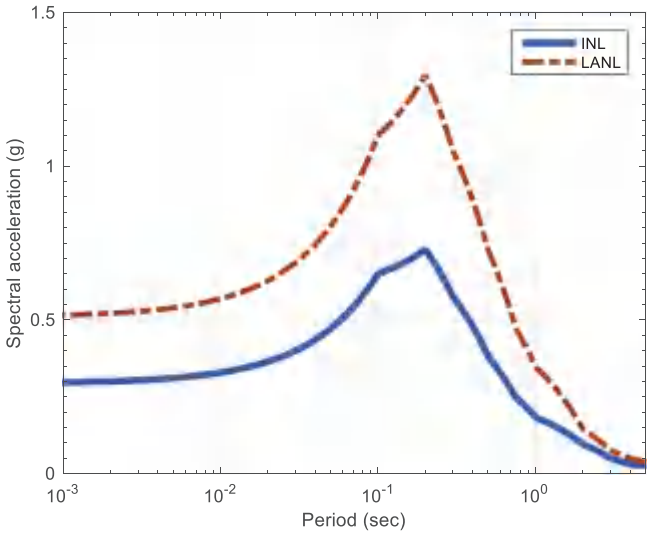

b. logarithmic scale

Fig. 3. Horizontal acceleration spectra for INL and LANL sites for a return period of 10,000 years and 5% damping: DBE shaking.

energy and reduces displacements in the isolated GNF. The lateral displacement-force relationship of LR isolator is presented in Fig. 6. The parameter Q_d in Fig. 6 is the characteristic strength, which is associated with the area and dynamic yield stress of the lead core; Y is the yield displacement of the lead core; K_e is the elastic stiffness; K_d is the post-yield stiffness; and K_{eff} is the effective stiffness at a user-specified lateral displacement.

The isolators are located beneath the shear walls; their spacing is limited to 25 ft. Fig. 7 presents the assumed locations of the 38 LR isolators. The seismic isolation system was designed for DBE shaking per the provisions of ASCE/SEI Standard 4-16 using an iterative process, and the equations and assumptions presented in Constantinou et al. (2007) and McVitty and Constantinou (2015). The product of the iterative analysis was one size of isolator for both the INL and LANL sites: 33 inches in diameter, central lead plug of 6 inches in diameter, 25 layers of 0.42-inch thick rubber, 24 0.2-inch thick shim plates, two 1.25-inch diameter end plates, and two 1.25-inch thick flange plates, for a total bearing height of 20 inches. This bearing has the following mechanical properties: K_e of 38 kip/in, K_d of 8.2 kip/in, Q_d of 30 kips, and K_{eff} of 23.3 (13.9) kip/in associated with 1.9 (4.8) inches D_D for INL (LANL) site. The effective periods of the isolation system are 1.7 s and 2.1 s for the INL and LANL sites, respectively. The rated displacement capacity of this isolator, manufactured by Dynamic Isolation System Inc., in Sparks, NV, is 22 inches, and the corresponding maximum axial force is 1100 kips (http://www.dis-Inc.com/technical.html, accessed on June 1, 2016).

Since the purposes of this study are to characterize the benefits of seismic isolation in nuclear facilities at a high level and to provide a roadmap for risk-based decision making regarding the use (or not) of seismic isolation, the locations of the isolators and their design was not optimized. These 38 LR isolators are modeled using MAT_SEISMIC_ISOLATOR (MAT197) available in LS-DYNA. (Sophisticated isolator models (e.g., Kumar et al., 2014) are not employed because the lateral displacements at both the INL and LANL sites are small by comparison with the rated displacement capacity of the bearing.)

Chapter 12 of ASCE/SEI Standard 4-16 requires the calculation of the 80%-ile (90%-ile) lateral displacement of the isolation system (at

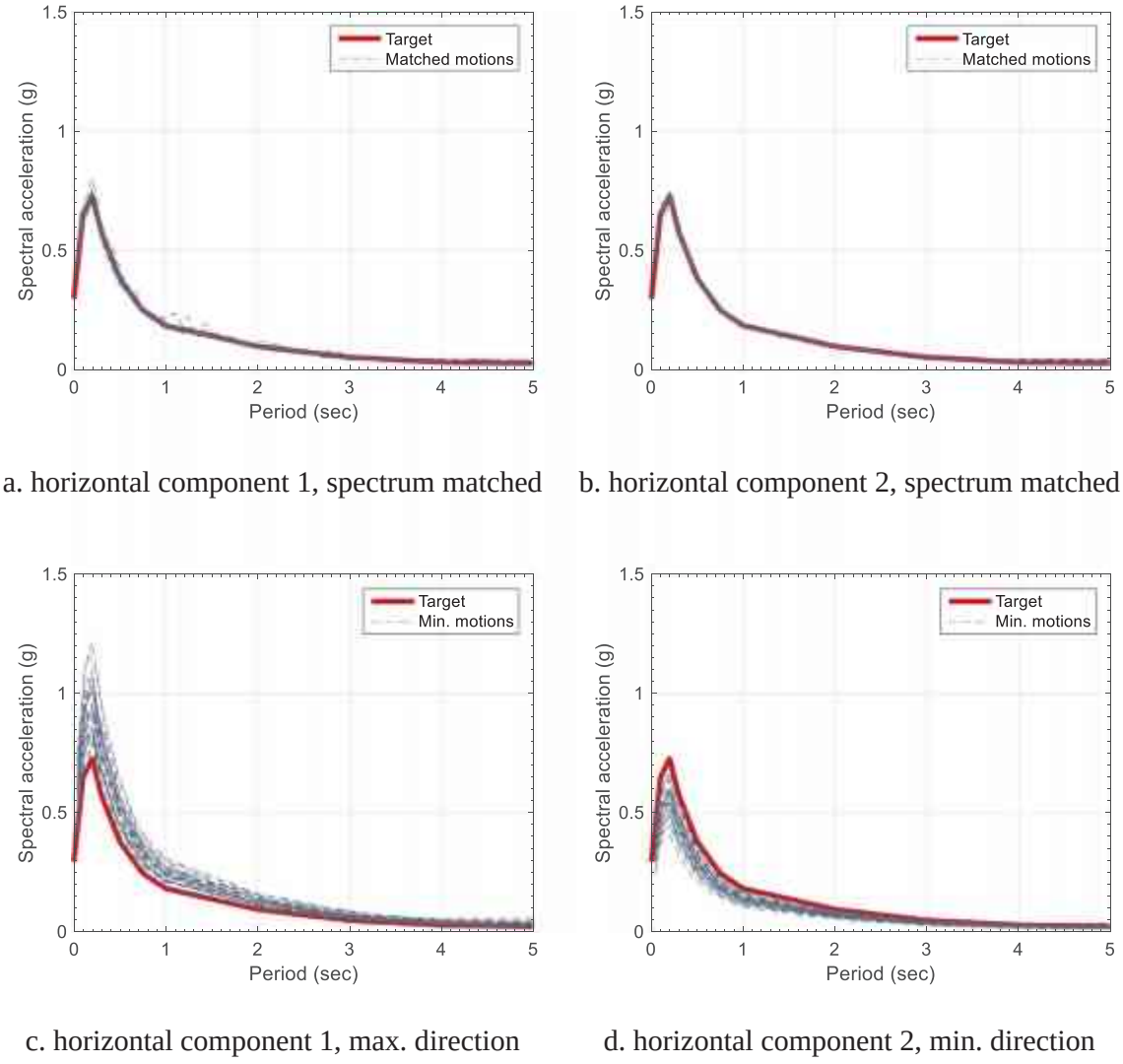

a. horizontal component 1, spectrum matched

b. horizontal component 2, spectrum matched

c. horizontal component 1, max. direction

d. horizontal component 2, min. direction

Fig. 4. Acceleration response spectra, INL, 5% damping: DBE shaking.

center of mass of the isolated superstructure, projected down to the basemat) for DBE shaking (150% DBE shaking). Because the base of the model is fixed against translation and rotation, the variability in the calculated displacements is due only to differences between the ground motions. (The variability in displacement response due to changes in the mechanical properties of the isolators is small by comparison with that due to ground motion (e.g., Huang et al., 2009b), and is not considered here.) The calculated displacements are listed in the third column of Table 2. The 80%-ile (90%-ile) compressive loads on the isolators (maximum compressive loads within all 38 isolators) with DBE shaking (150% DBE shaking) are listed in the fourth column of Table 2. The sizing of the LR isolator is controlled by the results of analysis for 150% DBE shaking at LANL site: the displacement of 13.9 inches is much less than the rated capacity of 22 inches and the compressive load of 913 kips is much less than the rated capacity at 22 inches lateral displacement of 1100 kips.

Chapter 12 of ASCE/SEI Standard 4-16 requires the provision of a stop (or displacement restraint) along the two horizontal axes of the isolated building at no less than the 90%-ile displacement in each direction from 150% DBE shaking. These displacements are listed in the fifth and sixth columns of Table 2 for the X and Y directions (see Fig. 1), respectively.

5. Seismic risk calculations

Seismic probabilistic risk assessment (SPRA) is used to compute the mean annual frequency of unacceptable performance, which would include core damage and large early radiation release for commercial nuclear power plants. The SPRA methodology used in this study is that proposed by Huang et al. (2008a, 2011a,b), which was developed to accommodate nonlinear elements in a soil-facility system, including nonlinear seismic isolators. Fig. 8 presents the five-step Huang SPRA methodology. This methodology is similar to industry-standard SPRA methods (EPRI, 2013) but with novel enhancements in the treatment of structural response, with emphasis on nonlinear soil-structure systems.

Step 1 involves a plant system analysis. Event trees and fault trees leading to an accident associated with unacceptable performance (e.g., core damage) are developed, by-and-large consistent with current practice (EPRI, 2013). Fragility curves for the SSCs contributing to the accident sequence are developed, with demands local to each component (e.g., story drift for a shear wall, spectral acceleration at 5 Hz at the point of attachment for a motor control center), rather than the traditional practice of indirectly linking local demands to a ground motion parameter such as peak horizontal ground acceleration in the free field via in-structure seismic demand estimates derived from stand-alone hazard-compatible structural response analyses.

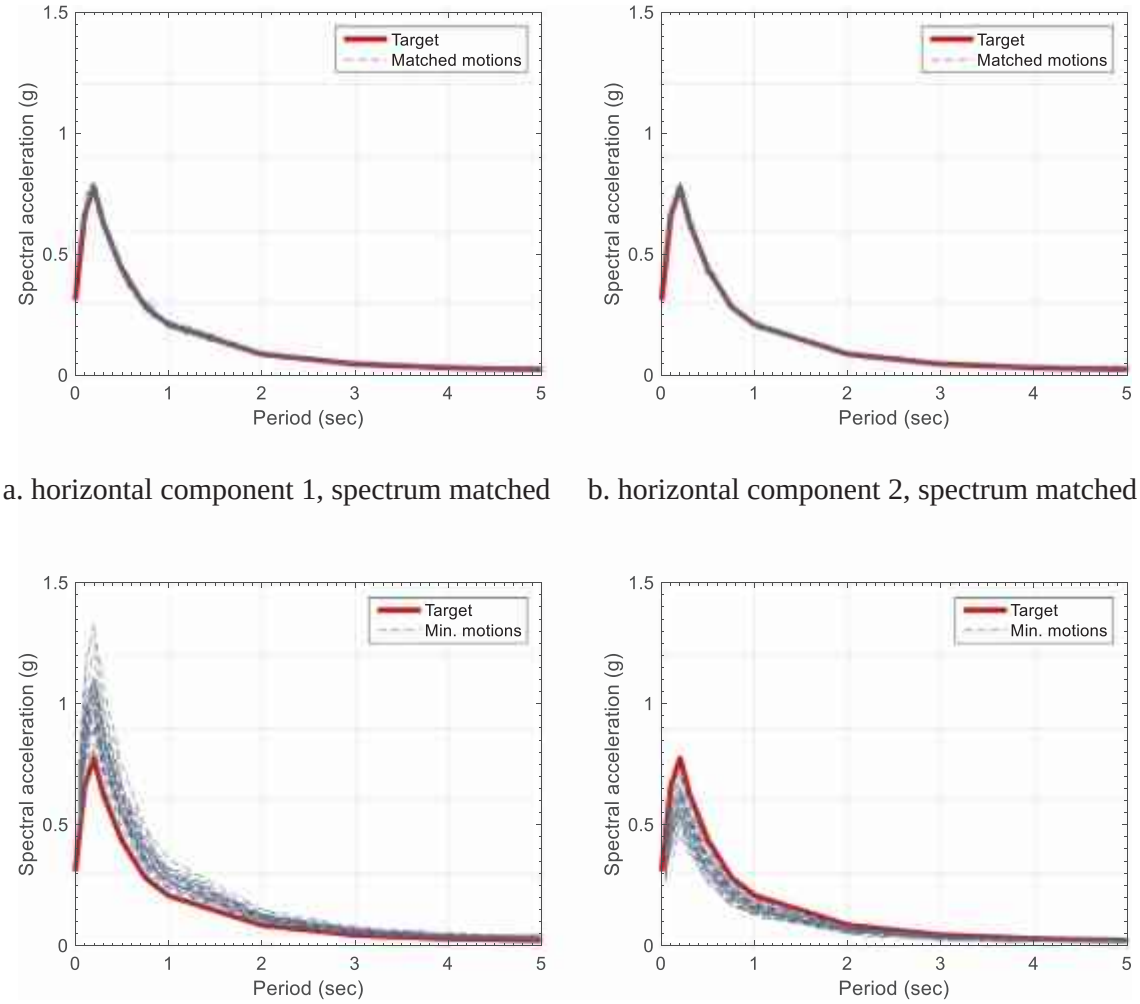

Fig. 5. Acceleration response spectra, LANL, 5% damping: DBE shaking.

Step 2 involves probabilistic seismic hazard analysis (PSHA). Seismic hazard curves, which are a product of PSHA, are generated for user-specified fundamental periods, which could be: 1) the fundamental period of the soil-structure system estimated for design basis earthquake shaking, 2) the fundamental translational period of the nuclear power plant superstructure, and 3) the first translational period of an isolated nuclear power plant, based on expected lateral displacements in design basis earthquake shaking. In Huang's methodology, the hazard curve is split into multiple intervals for response-history and risk calculations, where the intervals span the range of interest in risk space

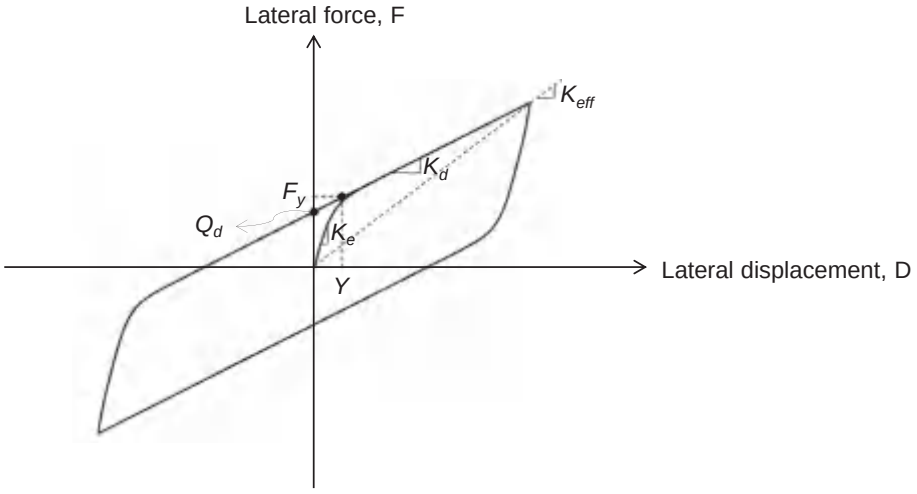

Fig. 6. Assumed lateral displacement-force relationship of a LR isolator.

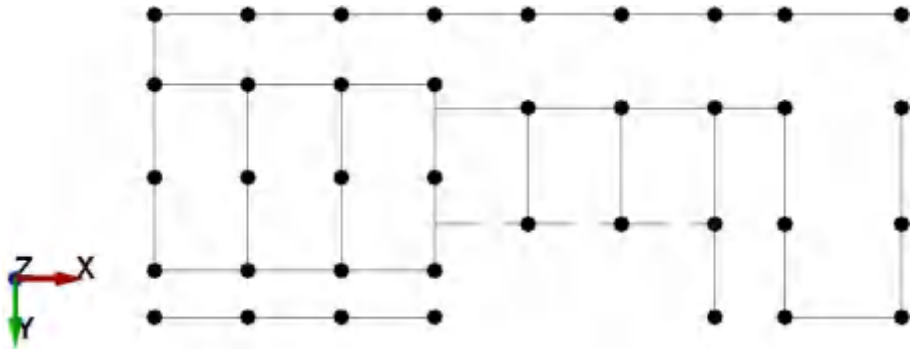

Fig. 7. Locations of LR isolators and global coordinate system.

Table 2
Horizontal displacement and axial compression load for DBE and 150% DBE shaking.

		Displacement at CM[1] (in)	Compressive load (kip)	Displacement along horizontal direction (in)	
				X[2]	Y[2]
INL	80%-ile, DBE shaking	4.1	841	–	–
	90%-ile, 150% DBE shaking	9.0	862	7.3	6.5
LANL	80%-ile, DBE shaking	7.5	869	–	–
	90%-ile, 150% DBE shaking	13.9	913	12.3	12.4

[1] Center of mass of the isolated superstructure, projected down to the basemat.
[2] Fig. 1 presents the coordinate system.

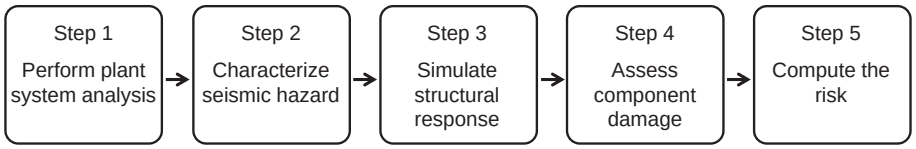

Fig. 8. SPRA methodology (Huang et al., 2008b, 2011a).

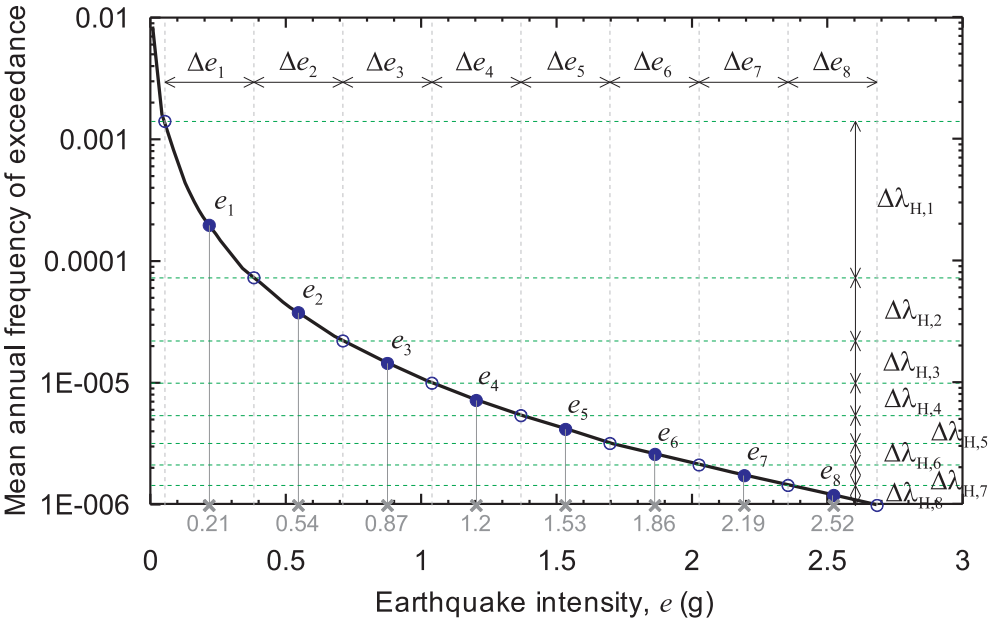

Fig. 9. Seismic hazard curve, midpoint spectral accelerations, and mean annual frequencies of occurrence (Huang et al., 2011a).

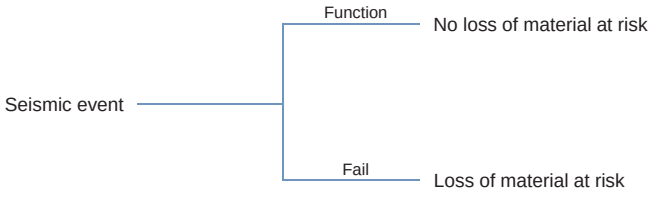

Fig. 10. Safety system event tree assumed for risk assessment.

(near zero conditional probability of unacceptable performance through 100% conditional probability of unacceptable performance), also largely consistent with current practice (EPRI, 2013). A sample hazard curve is presented in Fig. 9: each interval has a mid-point spectral acceleration ($S_{a,i} = e_i$) for the i-th intensity interval and a mean annual frequency of occurrence ($\Delta\lambda_i$). Ground motion time series are selected and scaled for each intensity level, and these are used for response-history analysis in the next step.

The ground motions of Step 2 are used in Step 3 to perform tens of nonlinear response-history analyses of the 3D model of the soil-structure or structural system. The demands on the SSCs at each of the intensities of shaking are then described by mean values, logarithmic standard deviations and cross correlation coefficients. Using a procedure developed by Yang et al. (2009) and implemented in FEMA P-58 (ATC, 2012), the tens of values of demand are replaced by tens of thousands of realizations of demand for Monte Carlo simulations. Step 4 uses the realizations of Step 3 and the fragility functions of Step 1 for systems analysis to identify the failure probability of the components. The product of this analysis, for each of the intensities of shaking, is a conditional probability of unacceptable performance. In Step 5, the conditional probability of unacceptable performance for each (mid-point) intensity of shaking, $S_{a,i}$, is multiplied by the corresponding mean annual frequency of occurrence of the shaking in the interval, $\Delta\lambda_i$, to calculate a contribution to the total seismic risk: a calculation also consistent with current SPRA practice in the United States.

5.1. Step 1: Plant system analysis

5.1.1. Event tree and fault tree

Systems and components that are generic to safety-related nuclear structures are used to populate the GNF and to perform the risk assessment. A single system is chosen for risk calculations. This system is intended to confine a loss of MAR to inside the structure. A highly simplified, hypothetical event tree is assumed for this system and is presented in Fig. 10, which shows that MAR will be lost to the atmosphere if the system fails in an earthquake.

A hypothetical fault tree for this system is presented in Fig. 11. There are three key SSC categories in the fault tree: confinement, mechanical components, and electrical components. There are a total of eight basic components in these three categories, chosen from EPRI (2013). The first column of Table 3 lists the components. Here, the building structure (component 6) is assumed to be framing that surrounds the pressure vessel. The nodes and locations of the SSCs are also listed in Table 3 and presented in Fig. 12.

The fault tree is simplistic and important interactions between mechanical and electrical systems, and electrical systems and active confinement (HVAC) are not considered. The notation ⌒ (AND) and ∩ (OR) gates in Fig. 11 describe the assumed path (and resistance) to a loss of MAR. The system is assumed to have failed if 1) confinement is lost, 2) mechanical components fail, or 3) electrical components fail.

5.1.2. Fragility curve of SSCs

Fragility curves must be developed to enable calculations of risk (or mean annual frequency of unacceptable performance). The cumulative

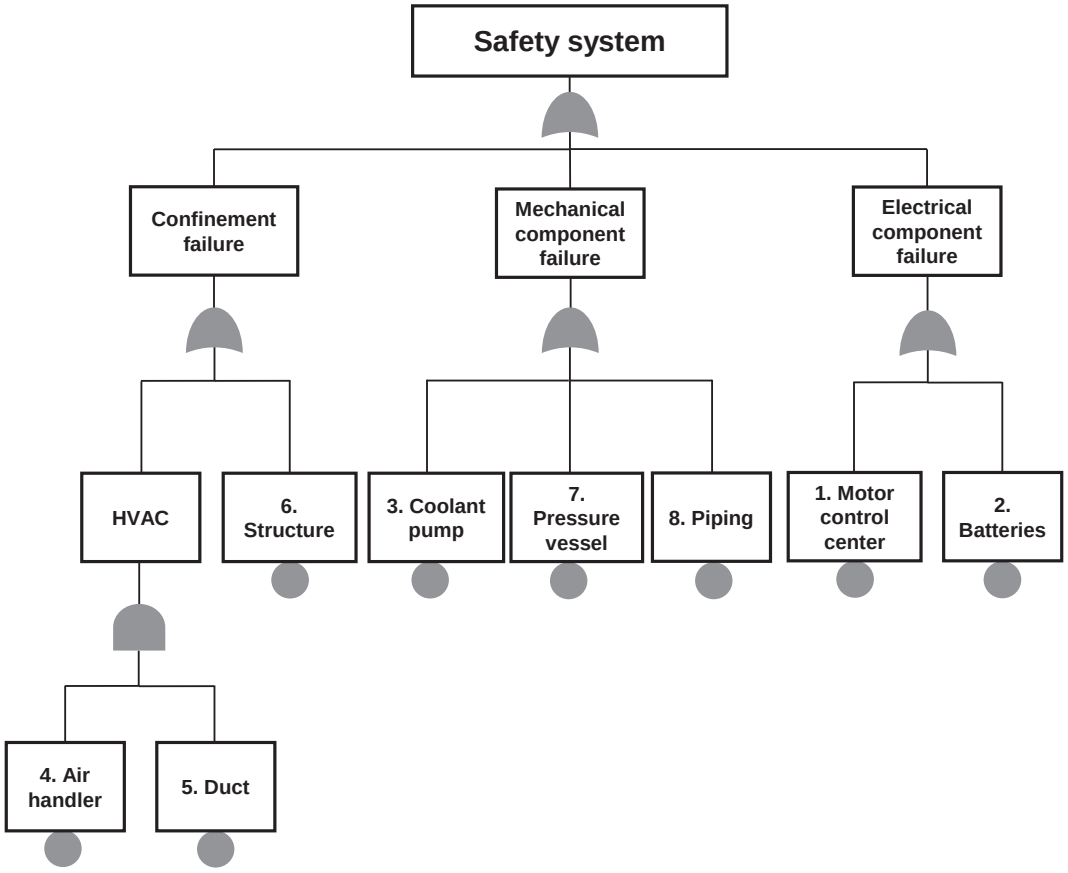

Fig. 11. Safety system fault tree assumed for risk assessment.

Table 3
SSCs, locations,[1] demands and frequency ranges.

Component	Node number	Location (ft.)			Frequency range (Hz)	Response parameter
		x	y	z		
1. Motor control center (MCC)	1712	30	65	10	3–10	Average S_a [2]
2. Battery	699	0	35	10	10–15	Average S_a
3. Coolant pump	278	50	34	−8	7–10	Average S_a
4. Air handler	744	15	15	5	10–20	Average S_a
5. HVAC duct	1085	95	25	25	2–20	Peak S_a
6. Structure (around vessel)	259	145	30	−8	5–10	Average S_a
	1898	145	30	25		
7. Pressure vessel	259	145	30	−8	10–33	Average S_a
8. Piping	778	40	50	25	4–33	Maximum peak S_a at all nodes
	1649	105	15	25		
	1665	65	15	25		

[1] The origin (0, 0, 0) is identified in Fig. 12 as a red circle.
[2] Spectral acceleration over frequency range.

lognormal distribution is widely used for describing fragility curves. The variable used to characterize fragility can vary by application, and has traditionally been peak ground acceleration, but should be a demand parameter that best characterizes the response of the component (e.g., floor spectral acceleration for some equipment, story drift for reinforced concrete shear walls). Fragility curves can be defined using a double lognormal model, which is a cumulative lognormal distribution with an uncertain median value, as presented in Eq. (1):

$$P_f(a) = \Phi\left[\frac{\ln(a/\bar{a})}{\beta_r}\right] \quad (1)$$

where $P_f(a)$ is the probability of failure of the component at a demand of a and Φ is the probability density function of the standard normal distribution. The aleatory variability (or randomness) is described by the logarithmic standard deviation β_r. The aleatory variability is inherent in the variable a, and cannot be reduced. Parameter $\bar{a}$ is the median (50%-ile) of the fragility and is used to characterize the capacity of the component, which follows cumulative lognormal distribution as follows:

$$\bar{a} = \hat{a} \cdot e^{-\Phi^{-1}(Q)\cdot\beta_u} \quad (2)$$

where $\hat{a}$ is the median value of the capacity of the component; β_u is the logarithmic standard deviation in the capacity of the component that describes the epistemic uncertainty associated with a lack of knowledge (and can be reduced), and Q is the probability of exceedance associated with a given capacity $\bar{a}$.

For this study, the assumed accident involves the eight SSCs listed in Table 3. Response-based fragility curves are developed for these SSCs. The fragility curve used here is the mean composite curve proposed by Reed and Kennedy (1994), which is the weighted average of all possible

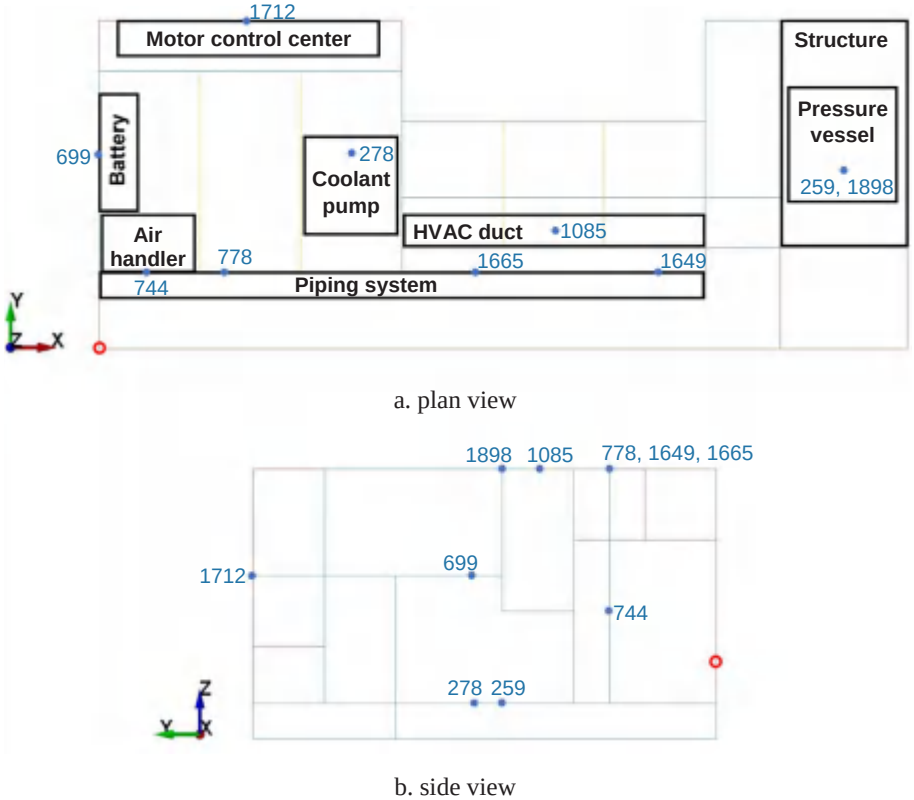

Fig. 12. Locations and nodes of SSCs in the GNF.

Table 4
SSC fragility definitions at INL and LANL.

Component	$\hat{a}$		β_u	β_r	β_c
	INL	LANL			
1. Motor control center (MCC)	14.5	28.3	0.30	0.35	0.46
2. Battery	4.0	7.4	0.30	0.35	0.46
3. Coolant pump	3.1	6.4	0.30	0.40	0.50
4. Air handler	3.4	6.3	0.30	0.40	0.50
5. HVAC duct	33.8	65.0	0.35	0.50	0.61
6. Structure (around vessel)	3.3	6.6	0.30	0.35	0.46
7. Pressure vessel	1.9	3.9	0.30	0.35	0.46
8. Piping	32.0	62.3	0.30	0.50	0.58

curves with different median values, $\bar{a}$. The mean fragility curve has a median defined by the median capacity, $\hat{a}$, and a composite logarithmic standard deviation, β_c, given by:

$$P_f(a) = \Phi\left[\frac{\ln(a/\hat{a})}{\beta_c}\right] \tag{3}$$

where the composite logarithmic standard deviation, β_c, is given by:

$$\beta_c = \sqrt{\beta_u^2 + \beta_r^2} \tag{4}$$

Values for the parameters $\hat{a}$, β_u, and β_r define a fragility curve. The value of a associated with a 95% confidence of a 5% failure probability is defined as the high-confidence-of-low-probability (HCLPF) capacity. Solving for a in Eq. (1) with P_f = 5% and assuming Q = 95% in Eq. (2) leads to a HCLPF capacity per Eq. (5):

$$HCLPF = \hat{a} \cdot e^{-1.65(\beta_r + \beta_u)} \tag{5}$$

For this study, the HCLPF capacities for the eight SSCs are attached to the median responses of the conventionally founded structure calculated by analysis using the 30 DBE ground motions, to ensure that component fragilities are reasonably consistent with minimum expected seismic performance in the United States. The chosen response quantity varies by component per column 7 in Table 3. The responses, which are all related to spectral acceleration for the SSCs selected here, are calculated at the locations shown in Fig. 12. Responses are calculated for a damping ratio of 2% of critical. The median value, $\hat{a}$, of the fragility curve can be back calculated from Eq. (5) given the HCLPF capacity and values for β_u and β_r .

EPRI (2013) proposes typical values of β_u and β_r for peak ground acceleration- (PGA-) based fragility curves for SSCs of nuclear structures. The values of β_u and β_r for PGA-based fragility curves include uncertainty in structure response. The risk calculations performed in this study use fragility curves characterized using local responses (e.g., average floor spectrum acceleration at the point of attachment) because demands on SSCs are calculated directly by response-history analysis. However, in this study, the typical values of β_u and β_r in EPRI (2013) are used to calculate β_c per Eq. (4) because 1) more directly applicable values are not readily available, and 2) the use of these values should not bias the relative risks in the conventionally founded and isolated buildings. Values of $\hat{a}$, β_u, β_r, and β_c for all the components of the GNF are presented in Table 4.

5.2. Step 2: Seismic hazard analysis

Hazard analysis is performed for the two sites: INL and LANL. The hazard curves of Fig. 2 are divided into 6 intensity intervals, with midpoint values identified by solid black and red circles. These intensities are multiples of DBE shaking: 0.5DBE, DBE, 1.5DBE, 2DBE, 2.5DBE, and 3DBE. The midpoint spectral accelerations, $S_{a,i}$, and the corresponding mean annual frequencies of occurrence, $\Delta\lambda_i$, are listed in Table 5. A set of ground motion acceleration time series is scaled to each of the midpoint spectral accelerations and used for response-history analysis in the next step.

5.3. Step 3: Structural response

Thirty pairs of horizontal max-min ground motions are used to perform response-history analysis of the conventional founded and base-isolated GNFs at each site. In-structure spectral accelerations of the ten nodes listed in Table 3 are calculated for a frequency range of 2 Hz to 33 Hz, assuming a damping ratio 2%, for both the conventionally founded and base-isolated buildings: the range associated

Table 5
Midpoint spectral accelerations, $S_{a,i}$, mean annual frequencies of occurrence, $\Delta\lambda_i$, and risk calculated using the simplified procedure.

a. INL

i	Conventionally founded building				Isolated building			
	$S_{a,i}$ (g)	$\Delta\lambda_i$	$P_{UP}(S_{a,i})$	$\Delta\lambda_i \times P_{UP}(S_{a,i})$	$S_{a,i}$ (g)	$\Delta\lambda_i$	$P_{UP}(S_{a,i})$	$\Delta\lambda_i \times P_{UP}(S_{a,i})$
1	0.33	2.16×10^{-3}	0.011	2.39×10^{-5}	0.05	3.19×10^{-3}	4.43×10^{-14}	1.42×10^{-16}
2	0.65	1.54×10^{-4}	0.240	3.69×10^{-5}	0.10	1.68×10^{-4}	1.61×10^{-11}	2.70×10^{-15}
3	0.98	3.53×10^{-5}	0.636	2.24×10^{-5}	0.15	3.55×10^{-5}	1.09×10^{-9}	3.88×10^{-14}
4	1.30	1.19×10^{-5}	0.878	1.05×10^{-5}	0.20	1.12×10^{-5}	1.82×10^{-8}	2.05×10^{-13}
5	1.63	4.78×10^{-6}	0.968	4.62×10^{-6}	0.24	4.28×10^{-6}	2.25×10^{-7}	9.61×10^{-13}
6	1.95	2.32×10^{-6}	0.993	2.31×10^{-6}	0.29	1.69×10^{-6}	1.36×10^{-6}	2.29×10^{-12}
	$\lambda_{UP} = \sum_{i=1}^{6} P_{UP}(S_{a,i}) \cdot \Delta\lambda_{H,i}$			1.01×10^{-4}	$\lambda_{UP} = \sum_{i=1}^{6} P_{UP}(S_{a,i}) \cdot \Delta\lambda_{H,i}$			3.50×10^{-12}

b. LANL

i	Conventionally founded building				Isolated building			
	$S_{a,i}$ (g)	$\Delta\lambda_i$	$P_{UP}(S_{a,i})$	$\Delta\lambda_i \times P_{UP}(S_{a,i})$	$S_{a,i}$ (g)	$\Delta\lambda_i$	$P_{UP}(S_{a,i})$	$\Delta\lambda_i \times P_{UP}(S_{a,i})$
1	0.55	7.94×10^{-4}	0.007	5.18×10^{-6}	0.07	6.97×10^{-4}	6.40×10^{-16}	4.46×10^{-19}
2	1.10	1.04×10^{-4}	0.203	2.11×10^{-5}	0.15	9.20×10^{-5}	1.51×10^{-12}	1.39×10^{-16}
3	1.65	3.50×10^{-5}	0.605	2.12×10^{-5}	0.22	3.33×10^{-5}	1.53×10^{-10}	5.08×10^{-15}
4	2.20	1.47×10^{-5}	0.861	1.26×10^{-5}	0.29	1.55×10^{-5}	3.79×10^{-9}	5.85×10^{-14}
5	2.75	7.21×10^{-6}	0.959	6.92×10^{-6}	0.36	8.28×10^{-6}	4.81×10^{-8}	3.98×10^{-13}
6	3.30	3.87×10^{-6}	0.989	3.82×10^{-6}	0.44	4.37×10^{-6}	3.57×10^{-7}	1.56×10^{-12}
	$\lambda_{UP} = \sum_{i=1}^{6} P_{UP}(S_{a,i}) \cdot \Delta\lambda_{H,i}$			7.09×10^{-5}	$\lambda_{UP} = \sum_{i=1}^{6} P_{UP}(S_{a,i}) \cdot \Delta\lambda_{H,i}$			2.02×10^{-12}

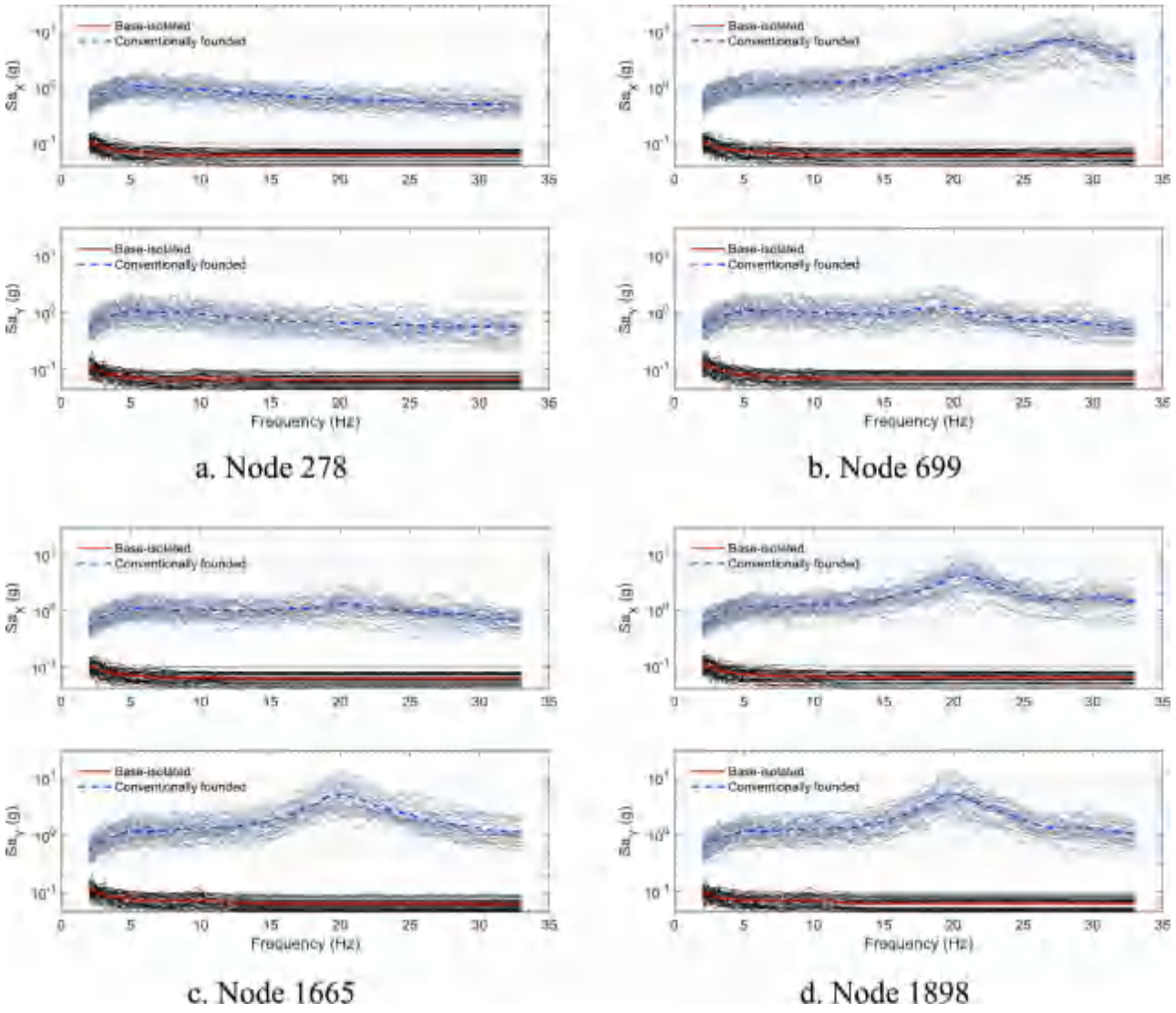

Fig. 13. In-structure acceleration response spectra, 2% damping, INL site.

with systems and components in nuclear facilities. Fig. 13 (Fig. 14) presents in-structure spectra for Node 278, Node 699, Node 1665, and Node 1898 in Fig. 12, in the X and Y directions, for the 30 DBE pairs of ground motions, together with the mean spectrum (dashed blue line for the conventionally founded building and solid red line for the base-isolated building), for the INL site (LANL site). The spectral accelerations in the (non-optimized) base-isolated building are much smaller than those in the conventionally founded building. The demands on the SSCs for the response parameters listed in the last column of Table 3 are calculated from these spectral accelerations and arranged in matrices, termed demand matrices. The size of the demand matrices is 30 × 8, where the number of row vectors is determined by the number of nonlinear response-history analyses for a given intensity of shaking and the number of columns is determined by the number of demands on the SSCs. Demand matrices are generated for 6 intensities of shaking in this study.

5.4. Step 4: Component damage assessment

Two procedures are used here to estimate the probability of unacceptable performance conditioned on an intensity of earthquake shaking: 1) a simplified method based on Boolean algebra and probability theory, and 2) the rigorous Monte Carlo procedure presented in Huang et al. (2008a, 2011a,b).

5.4.1. Simplified procedure

The simplified procedure utilizes Boolean algebra and basic probability theory. Fig. 11 and the following text explain the simplified procedure.

In Fig. 11, the Boolean notation $\cap$ denotes conjunction ($\wedge$ or AND) and $\cup$ denotes disjunction ($\vee$ or OR). In this fault tree, failure of a component/event immediately above an AND gate requires failure of all the components/events immediately below the gate. The failure of a component/event immediately above an OR gate requires failure of one or more components/events immediately below the gate. The failure probability of the components/events in the fault tree can be calculated using the failure probability of each sub-component ($P_{f,i}$, i = the number of component). In the fault tree of Fig. 11, and assuming independence of components 1 through 8, the failure probability of the HVAC system is ($P_{f,4} \times P_{f,5}$) and of the electrical component is ($P_{f,1} + P_{f,2} - P_{f,1} \times P_{f,2}$). The conditional probability of unacceptable performance $P_{UP}(S_{a,i})$ for shaking associated with spectral intensity $S_{a,i}$ can be calculated using the failure probability, $P_f(a)$, of each SSC. The fragility function for the SSC and demand on the SSC computed by nonlinear response-history analysis are used to calculate the failure probability, $P_f(a)$. Thirty values of failure probability are computed for each SSC at each level of shaking. The fault tree in Fig. 11 is then used, in conjunction with probability theory, to compute the conditional probability of unacceptable performance on each of 30 nonlinear

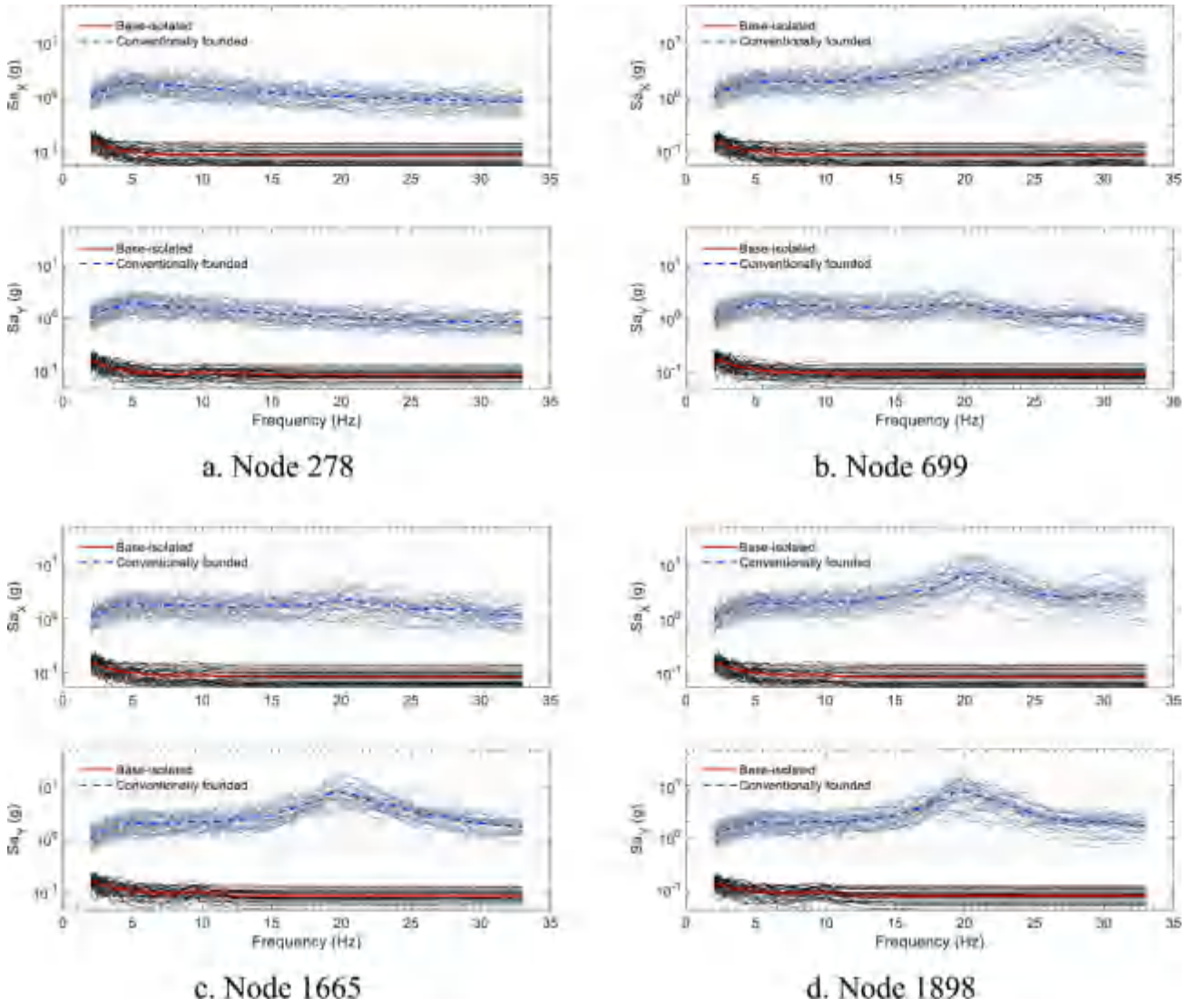

Fig. 14. In-structure acceleration response spectra, 2% damping, LANL site.

response-history analyses. The conditional probability of unacceptable performance, $P_{UP}(S_{a,i})$, at the chosen intensity of shaking is the average of the 30 values. The values of $P_{UP}(S_{a,i})$ for conventionally founded and base-isolated building are presented in Table 5 for both sites.

5.4.2. Monte Carlo procedure

Monte Carlo-based risk assessment requires the use of 100 s to tens of 1000 s of realizations for each level of earthquake shaking intensity. It is computationally expensive to run tens of 1000 s of simulations, especially when nonlinear soil is included in the numerical model, and the available number of seed earthquake ground motions to be used as inputs is too small. Accordingly, the procedure developed by Yang et al. (2009) and implemented in FEMA P-58 is used to generate tens of 1000 s of realizations. The procedure assumes that demands on the SSCs follow the lognormal distribution and it maintains in the much larger set of realizations the underlying statistics (mean values, logarithmic standard deviations and cross correlation coefficients) of the SSC demands calculated by nonlinear response-history analysis. A procedure based on central limit theorem is used to determine the number of row vectors, N, needed to obtain an accurate estimate of the conditional probability of unacceptable performance at each level of shaking. The size of the augmented demand matrices is $N \times 8$.

Monte Carlo simulations are used to assess the status of an SSC: functional or failed. For each SSC, a random number is picked from a uniform distribution between 0 and 1 and compared to its failure probability, $P_f(a)$. If the random number is smaller than or equal to $P_f(a)$, the SSC is considered to have failed; otherwise it is considered to be functional. The process is repeated for all SSCs for one row of the augmented demand matrix ($N \times 8$ here), to determine the damage status of each SSC for the realization. The SSC damage status, the fault tree of Fig. 11, and the component/event relationships defined by the Boolean algebra, are then used to determine whether the performance is acceptable for the realization. The result from each realization is a Bernoulli random variable since the only outcomes are either occurrence or non-occurrence. The process is repeated for all realizations in the augmented demand matrix and the total number of occurrences of unacceptable performance, n_{UP}, is recorded for that level of shaking intensity. The conditional probability of unacceptable performance, $P_{UP}(S_{a,i})$, at the chosen intensity of shaking, is given by:

$$P_{UP}(S_{a,i}) = \frac{n_{UP}}{N} \tag{6}$$

where the variables were defined previously. The values of $P_{UP}(S_{a,i})$ for conventionally founded and base-isolated building are presented in Table 6 for both sites.

Table 6
Midpoint spectral accelerations, $S_{a,i}$, mean annual frequencies of occurrence, $\Delta\lambda_i$, and risk calculated by Monte Carlo analysis.

a. INL

i	Conventionally founded building				Isolated building			
	$S_{a,i}$ (g)	$\Delta\lambda_i$	$P_{UP}(S_{a,i})$	$\Delta\lambda_i \times P_{UP}(S_{a,i})$	$S_{a,i}$ (g)	$\Delta\lambda_i$	$P_{UP}(S_{a,i})$	$\Delta\lambda_i \times P_{UP}(S_{a,i})$
1	0.33	2.16×10^{-3}	0.013	2.08×10^{-5}	0.05	3.19×10^{-3}	0	0
2	0.65	1.54×10^{-4}	0.233	3.58×10^{-5}	0.10	1.68×10^{-4}	0	0
3	0.98	3.53×10^{-5}	0.618	2.18×10^{-5}	0.15	3.55×10^{-5}	1.67×10^{-9}	5.92×10^{-14}
4	1.30	1.19×10^{-5}	0.895	1.07×10^{-5}	0.20	1.12×10^{-5}	2.10×10^{-8}	2.36×10^{-13}
5	1.63	4.78×10^{-6}	0.973	4.65×10^{-6}	0.24	4.28×10^{-6}	5.16×10^{-7}	2.21×10^{-13}
6	1.95	2.32×10^{-6}	0.987	2.29×10^{-6}	0.29	1.69×10^{-6}	3.07×10^{-6}	5.18×10^{-12}
		$\lambda_{UP} = \sum_{i=1}^{6} P_{UP}(S_{a,i}) \cdot \Delta\lambda_{H,i}$		1.03×10^{-4}		$\lambda_{UP} = \sum_{i=1}^{6} P_{UP}(S_{a,i}) \cdot \Delta\lambda_{H,i}$		7.69×10^{-12}

b. LANL

i	Conventionally founded building				Isolated building			
	$S_{a,i}$ (g)	$\Delta\lambda_i$	$P_{UP}(S_{a,i})$	$\Delta\lambda_i \times P_{UP}(S_{a,i})$	$S_{a,i}$ (g)	$\Delta\lambda_i$	$P_{UP}(S_{a,i})$	$\Delta\lambda_i \times P_{UP}(S_{a,i})$
1	0.55	7.94×10^{-4}	0.008	6.39×10^{-6}	0.07	6.97×10^{-4}	0	0
2	1.10	1.04×10^{-4}	0.207	2.15×10^{-5}	0.15	9.20×10^{-5}	0	0
3	1.65	3.50×10^{-5}	0.600	2.10×10^{-5}	0.22	3.33×10^{-5}	1.67×10^{-10}	5.55×10^{-15}
4	2.20	1.47×10^{-5}	0.880	1.29×10^{-5}	0.29	1.55×10^{-5}	4.83×10^{-9}	7.48×10^{-14}
5	2.75	7.21×10^{-6}	0.957	6.90×10^{-6}	0.36	8.28×10^{-6}	6.48×10^{-8}	5.37×10^{-13}
6	3.30	3.87×10^{-6}	0.993	3.84×10^{-6}	0.44	4.37×10^{-6}	4.68×10^{-7}	2.04×10^{-12}
		$\lambda_{UP} = \sum_{i=1}^{6} P_{UP}(S_{a,i}) \cdot \Delta\lambda_{H,i}$		7.25×10^{-5}		$\lambda_{UP} = \sum_{i=1}^{6} P_{UP}(S_{a,i}) \cdot \Delta\lambda_{H,i}$		2.66×10^{-12}

5.5. Step 5: Seismic risk computation

The seismic risk (or annual frequency of unacceptable performance), λ_{UP}, is the sum of the products of $P_{UP}(S_{a,i})$ and the corresponding $\Delta\lambda_i$:

$$\lambda_{UP} = \sum_{i=1}^{6} P_{UP}(S_{a,i}) \cdot \Delta\lambda_{H,i} \tag{7}$$

Results of the risk calculations are presented in Table 5 (Boolean-based procedure) and Table 6 (Monte Carlo procedure). Identical SSCs are used in both the conventionally founded and base-isolated buildings for each site, but with different fragility curves at each site because design basis earthquake shaking at LANL is more intense than at INL, as described previously.

5.6. Discussion

The Monte Carlo-based probability of unacceptable performance in the base-isolated GNF, at the two lowest intensities of shaking, $S_{a,1}$ and $S_{a,2}$, is zero at both sites. Non-zero values are calculated using the simplified procedure. The addition of many more realizations to the demand matrices would result in non-zero probabilities for the Monte Carlo analysis at these intensities of shaking. However, it is evident from the results of Table 5 that the contribution to the mean annual frequency of unacceptable performance of the isolated SSCs from the two lowest levels of earthquake shaking is tiny, making it unnecessary to augment the demand matrix and perform additional calculations.

Regardless of whether the simplified or the Monte Carlo procedure is used to calculate risk, it is evident that the introduction of seismic isolation reduces the mean annual frequency of unacceptable performance by many orders of magnitude: to values too small to have physical significance (return periods of the order of 1000 times the age of the Earth). A comparison of results from both Tables 5 and 6 make this clear. The risk will increase to both the conventionally founded and base-isolated GNF if vertical shaking is considered, but those calculations are not possible because fragility functions that address such shaking are not available. Importantly, the same SSCs were used in both the conventionally founded and base-isolated buildings, which prompted the study described in Section 7 below.

A comparison of results in Tables 5 and 6 show that the simplified procedure produced estimates of risk that are comparable to those computed by Monte Carlo analysis, at a very much lower computational expense. Although conclusive statements cannot be drawn based on a small number of analyses and very simple event and fault trees, the simplified procedure likely should have an important role to play in seismic probabilistic risk assessment, especially in the early phases of the design of a nuclear facility, when equipment layout and design has not been finalized, and reliable fragility functions are not yet available. Further, infusing risk calculations into the design process, from the beginning, will aid decision-making and ensure that performance goals are met. Further studies are needed to confirm the utility of the simplified procedure described here.

The calculated mean annual frequencies of unacceptable performance for the conventionally founded GNF, sited at both INL and LANL, are relatively high with respect to the target performance goals set forth in ASCE/SEI Standard 43-05 (ASCE, 2005). This is due to two factors, neither of which materially affects the key conclusions of this study: 1) the use of uniform hazard response spectra (UHRS) for design, anchored to a return period of 10,000 years, rather than a design response spectra (DRS) per ASCE 43-05, with ordinates greater than those of the UHRS by a design factor selected to meet the target performance goal, and 2) the use of a highly simplified event tree, as described earlier. The use of DRS rather than UHRS for developing the fragility curves for the SSCs will increase both the OCC and the cost of the SSCs, with the greatest increases at the INL site. Kumar et al. (2015, 2017) show that the design factor is equal to 1.0 for isolated structures, namely, the ordinates of the DRS and the UHRS are identical, and so a similar correction is not needed for the isolated building at either INL or LANL. (Importantly, the mean annual frequencies of unacceptable performance of the isolated GNF at the INL and LANL sites meet target performance goals by many orders of magnitude.)

The conditional probability of unacceptable performance for DBE shaking (i = 2 in Tables 5 and 6) and the conventionally founded GNF is greater at INL (moderate seismic hazard) than LANL (high seismic hazard): a counter-intuitive outcome. This is attributed to the two

factors identified in the previous paragraph.

The risk calculations for the conventionally founded GNF used seismic hazard curves anchored to a period of 0.10 s. This period corresponds to a translational mode with a low modal effective mass. Risk calculations were also performed for anchor periods of 0.0 s (i.e., peak ground acceleration) and 0.05 s. Results are reported in Appendix A. There are no appreciable changes to the calculated risk for the conventionally founded GNF, at either the INL or LANL site, if these alternate anchor periods are used.

6. Risk calculations for the isolation systems

The risk calculations in Section 5 focus on the safety-related SSCs in the GNF. Failure of the isolation system will contribute to the mean annual frequency of unacceptable performance of the base isolated GNF.

Kumar et al. (2015, 2017) present a procedure to calculate the seismic risk associated with the isolation system, and generated results for the INL and LANL sites, and that information is adopted here. Kumar et al. performed calculations using performance goals for an isolation system presented in ASCE/SEI Standard 4-16 for DOE facilities and the forthcoming NUREG (Kammerer et al., forthcoming) for commercial nuclear power plants. Both documents require: 1) all production isolators be tested for DBE demands, as calculated by analysis, 2) prototype isolators be tested to a lateral displacement corresponding to 90%-ile beyond DBE shaking (BDBE shaking) with coexisting maximum (compression) and minimum (perhaps tension) axial forces, and 3) a stop (or a displacement restraint) at the displacement of no less than the 90%-ile BDBE displacement. The key difference between the provisions of ASCE 4-16 and the draft NUREG is the definition of the BDBE: 150% DBE shaking in ASCE 4-16, and a uniform hazard spectrum with a mean annual frequency of exceedance of 10^{-5} in the NUREG.

The mean annual frequency of unacceptable performance of the isolation system calculated using the requirements of Chapter 12 of ASCE 4-16 at the INL and LANL sites is 1×10^{-6} and 2.1×10^{-6}, respectively, assuming a stop is provided and the prototype isolators are shown to perform adequately at 95% confidence at the 90%-ile BDBE displacement. These risk numbers are extremely conservative (high) because 1) isolator demands are assumed to be fully correlated, 2) isolation system failure is assumed to correspond to the failure of a single isolator (which is not possible due to the presence of a thick basemat above the isolation plane), and 3) the rated capacity of the LR isolator chosen here (see Table 2) is much greater than the 90%-ile demand at both the INL and LANL sites. If these three issues are addressed, the mean annual frequency of failure of the isolation system will likely reduce by orders of magnitude, to extremely small numbers. However, these failure frequencies will likely be four to five orders of magnitude greater than those of the SSCs in the isolated GNF per Tables 5 and 6, which enables a substantial increase in risk to the SSCs to the order of the failure frequency of the isolation system, with no meaningful change in the total risk in the isolated GNF.

7. Cost study

The cost of constructing safety-related nuclear facilities is driven in significant part by considerations of the effects of earthquake shaking, especially in commercial nuclear power plants. Capital cost can likely be reduced by the use of advanced numerical tools such as those for nonlinear site-response (e.g., Bolisetti et al. 2014), soil-structure interaction analysis (e.g., Coleman et al., 2015), and advanced probabilistic risk assessment (e.g., Huang et al., 2008a, 2011a, 2011b; Bolisetti et al., 2015; Coleman et al., 2016). Another strategy to decrease capital costs is to substantially reduce seismic demands required for seismic qualification of systems and components, which can be accomplished using seismic isolation and damping systems.

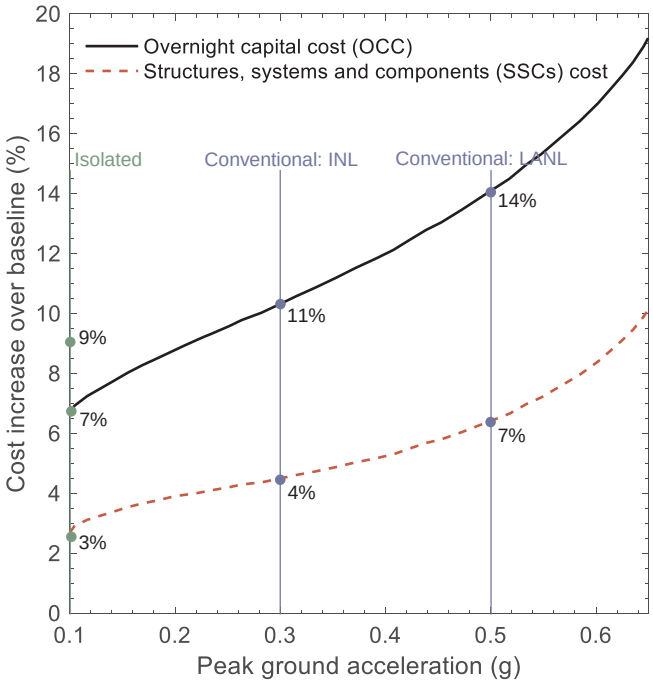

Fig. 15. Increase in cost as a percentage of OCC of the baseline design.

Table 7
Incremental cost[1] in OCC and SSCs mapped from Fig. 15 for the conventionally founded and base-isolated GNF at INL and LANL.

Incremental cost (million USD)	INL site		LANL site	
	Conventionally founded	Base-isolated	Conventionally founded	Base-isolated
OCC	11%	9%[2]	14%	9%[2]
SSCs	4%	3%[3]	7%	3%[3]

[1] Incremental cost as a percentage of the OCC of the baseline GNF.
[2] Includes $10 million USD for implementing isolation, approximately 2% of the $550 million USD cost of the baseline design.
[3] Cost of isolation not included in the SSCs.

Despite the broad agreement in the nuclear community that consideration of earthquake effects adds substantially to the cost of nuclear facilities, only one relatively comprehensive study has been performed on the subject to the knowledge of the authors. This study was first published as a NUREG report (Stevenson, 1981) and later updated (Stevenson, 2003) and it focused on the cost of building a 1200 MW light water reactor power plant. Because the Stevenson studies provide the most comprehensive known source of data that relates increase in plant cost to increase in seismic qualification demands, they are used for this study and are assumed to be 1) still current, and 2) applicable to a broad range of safety-related nuclear facilities, such as the GNF discussed here.

Herein, incremental seismic-related costs are estimated for 1) the overnight capital cost (OCC) of the GNF, and 2) the cost of the SSCs assumed in the GNF for both the conventionally founded and base-isolated conditions. A purpose of this study is to identify the benefits of seismic isolation as measured by reduced cost.

7.1. Overnight capital cost and SSC cost

The overnight capital cost (OCC) is the total cost of a facility excluding indirect costs such as cost escalation and interest during the

construction period. INL staff estimated the baseline OCC (i.e., design with no consideration of seismic loadings) for the GNF to be $550 million USD in 2016.

Stevenson (1981) binned the total cost of a large light water reactor into the categories of 1) site preparation and foundation, 2) building structures, 3) mechanical components, 4) electrical components, 5) distribution systems, and 6) engineering cost, and then estimated the supplemental cost for each bin associated with seismic design (or seismic considerations). Structures, systems and components were assumed to be represented by categories 2, 3, 4 and 5. Stevenson (2003) reported increases in OCC associated with considerations of earthquake shaking, above the baseline, of between 7% at a peak ground acceleration (PGA) of 0.1 g and 20% at a PGA of 0.65 g; see the solid line in Fig. 15. The dashed line in the figure is an estimate of the increase in cost over the baseline of the SSCs due to considerations of earthquake shaking, anchored to data in the NUREG (Stevenson, 1981). Also shown in the figure are the PGAs for the INL (= 0.3 g) and LANL (= 0.5 g) sites, and the corresponding percentage increases in cost (OCC and SSC) associated with seismic design and construction. The increases in the OCC over the baseline are 11% and 14%, or, $61 and $77 million USD, at the INL and LANL sites, respectively. The corresponding increases in the cost of the SSCs are 4% and 7% (or $22 and $39 million USD) at the INL and LANL sites, respectively. These estimated costs are listed in the second and fourth columns of Table 7.

Structures, systems and components in the base-isolated GNF will also be designed for the effects of earthquake shaking. Per the data in Figs. 13 and 14 for node 278 (on the basemat above the isolators), the mean peak floor acceleration (taken here as the spectral acceleration at a frequency of 33 Hz) on the basemat in the base-isolated GNF will be less than 0.1 g for both sites. However, that value is used here to characterize nominal minimum seismic qualification demand in the isolated GNF: the assumed percentage increases in cost mapped from Fig. 15 at this spectral acceleration are 3% (SSCs) and 7% (OCC). Additional design and construction effort is needed to implement the isolation system: 1) design, procurement and installation of the isolators (less than $0.75 million USD for the generic nuclear facility considered here), 2) over excavation to accommodate the additional foundation and pedestals, and 3) construction of the reinforced concrete foundation, moat walls and pedestals. These costs are estimated to be $10 million USD, which is approximately 2% of the OCC of the baseline GNF of $550 million USD. Not addressed here are the potential significant savings associated with the use of isolation in terms of seismic qualification: if in-structure spectral demands can be reduced to the levels shown in Figs. 13 and 14, qualification may be unnecessary.

The incremental OCC and SSC costs for the base-isolated GNF are listed in the third and fifth columns of Table 7. The incremental OCC cost includes the assumed $10 million USD required to construct the isolation system. But the incremental SSC cost does not.

The increase in cost associated with considerations of earthquake shaking are reduced by the use of seismic isolation to 2% (OCC) and 1% (SSCs) of the baseline OCC at the site of moderate seismic hazard (INL) and to 5% (OCC) and 4% (SSCs) at the site of high seismic hazard (LANL): values based on Stevenson's data. Anecdotal evidence collected by the authors in the past two years suggests that the seismic cost penalties estimated by Stevenson more than 20 years ago are low, indicating that the economic benefits of implementing seismic isolation would be much greater if contemporary cost data was used.

8. Summary and conclusions

This study provides a framework for assessing the benefits of seismic isolation and exercises the framework on a generic nuclear facility (GNF). The GNF is a two-story reinforced concrete building, with plan dimensions of 65 ft. × 160 ft. At its highest point, the GNF is approximately 38 ft. tall. Two potential benefits of seismic isolation considered herein are 1) increase in safety (or reduction in risk), and 2) a reduction in OCC and the cost of SSCs. The baseline cost of the GNF, excluding considerations of earthquake shaking effects, is approximately $550 million in 2016 USD.

The GNF is assumed to handle materials at risk (MAR). Sample SSCs in safety-related nuclear structures are used to populate the GNF. The SSCs are chosen from EPRI (2013), and include 1) motor control center (MCC), 2) battery, 3) coolant pump, 4) air handler, 5) heating, ventilation, air conditioning (HVAC) duct, 6) structure (surrounds the pressure vessel), 7) pressure vessel, and 8) piping. Calculations of risk and cost are performed for the sites of the Idaho National Laboratory (INL) and the Los Alamos National Laboratory (LANL), representing moderate and high seismic hazard, respectively, to generalize the outcomes of the study.

The eight SSCs are combined into three categories for risk calculations: confinement, mechanical and electrical. The SSCs are distributed over the footprint and height of the GNF. The fault tree is simplistic and important interactions between mechanical and electrical systems, and electrical systems and active confinement (HVAC) are not considered. The system is assumed to have failed if 1) confinement is lost, 2) mechanical components fail, or 3) electrical components fail. Representative fragility functions are assigned to each SSC using EPRI (2013) data as input.

Nonlinear dynamic analysis is used to calculate demands on structures, systems and components (SSCs) in the GNF. Thirty sets of earthquake ground motions, appropriately selected and scaled to represent design basis earthquake shaking (DBE), and multiples of DBE shaking, at the INL and LANL sites, are used for analysis. (Vertical earthquake shaking was not considered because representative SSC fragility data available for this component of input are less rigorous.) Results of simulations at multiple levels of earthquake shaking are used for seismic probabilistic risk assessment.

Seismic probabilistic risk assessment (SPRA) is performed using the five-step methodology proposed by Huang et al. (2008a, 2011a, 2011b), which can directly accommodate nonlinear elements in the soil-structure system. Two methods are used for assessment of component damage: 1) simplified Boolean, and 2) Monte Carlo. The two procedures generate similar values of the mean annual frequency of unacceptable performance of the GNF at a given site (i.e., INL or LANL) and boundary condition (i.e., conventionally founded or base-isolated). Although only demonstrated for one building at two sites, and for two different boundary conditions, the simplified Boolean-based method would appear to be viable for use in the early stages of a nuclear-facility design, to inform decision makers regarding the likely level of risk, and if too high or low, information on which SSCs to make design changes to so as to achieve specified performance goals.

The calculated mean annual frequency of release of MAR associated with the failure of SSCs is reduced by many orders of magnitude if seismic isolation is employed. The seismic risk associated with the failure of the isolation system is much greater that of the SSCs in the isolated facility but orders of magnitude smaller than the seismic risk in the conventionally founded GNF. Decreasing the ruggedness of the SSCs in the isolated GNF to provide seismic risk of the same order as that of the isolation system will be associated with significant reductions in SSC cost, which will vary by component. The mean annual frequency of release of materials at risk from the GNF is reduced by orders of magnitude, at both the INL and LANL sites, if the building is seismically isolated.

Cost calculations for the conventionally founded and base-isolated GNF are prepared using results and data from Stevenson (1981, 2003): the most current and comprehensive data available to the authors on the cost penalty associated with considerations of earthquake shaking in nuclear facility design. Stevenson calculated 1) the increase in overnight capital cost (OCC) of a large light-water reactor for design peak (horizontal) ground accelerations (PGAs) of between 0.1 g and 0.65 g, and 2) the cost of including earthquake shaking effects in the deployment and seismic design of various categories of SSCs in the

plant. The Stevenson data and the calculations performed here show that seismic base isolation would reduce the OCC of the GNF at both the INL and LANL sites.

This study demonstrates that seismic isolation of nuclear facilities has the potential to achieve both improved safety (lower risk) and reduced overnight capital cost.

Appendix A. Supplemental risk calculations for the conventionally founded GNF

Calculations of risk, measured here in terms of mean annual frequency of unacceptable performance, utilize a seismic hazard curve, which is anchored to a representative translational period of the facility being assessed. Table 1 identifies the horizontal translational modes in the GNF with significant modal effective mass: the corresponding frequencies are 20 Hz and greater. The risk calculations presented in the body of the paper use a seismic hazard curve for a period of 0.1 s. This period was chosen because the USGS provides hazard curves for the INL and LANL sites at this period. Hazard curve data for the sites at 0.05 s are not provided. To judge the importance of anchor period on the calculated risk, calculations are presented here using hazard curves at 0.0 s (PGA, provided by the USGS) and 0.05 s (20 Hz, interpolated from data at 0.0 and 0.10 s). The interpolation at 0.05 s was performed using log scaling for mean annual frequency of exceedance and linear scaling for spectral acceleration.

Fig. A1 presents seismic hazard curves for 5% damping at PGA, 0.05 and 0.1 s at both sites, together with solid circles on each curves representing mid-point spectral accelerations ($S_{a,i} = e_i$) for six ground motion intensity levels and the corresponding mean annual frequencies of occurrence ($\Delta\lambda_i$) defined in Fig. 9. Table A1 presents values of $\Delta\lambda_i$, the mean annual frequency of unacceptable performance, λ_{UP}, for the three hazard definitions and the two calculation procedures (i.e., simplified or Boolean-based, and Monte Carlo), and the percentage differences from the values reported in Tables 5 and 6.

The percentage differences in $\Delta\lambda_i$ are less than 10% for 0.05-s hazard curve at all intensity levels and generally much less than 10% for the PGA-based hazard curves. The percentage differences in the calculated risks are less than 5% if the PGA-based hazard curves are used, and less than 1% if the 0.05-s hazard curves are used. These results are insignificant in risk space and show the lack of sensitivity to calculated risk to the chosen seismic hazard curves, within the range considered here for the conventionally founded GNF.

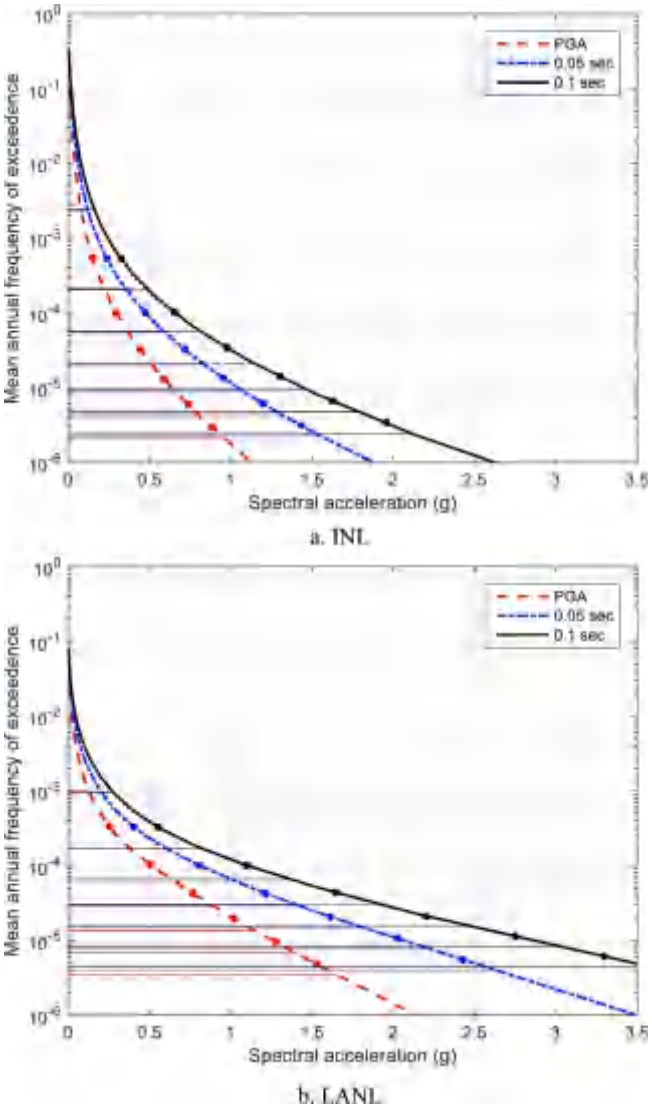

Fig. A1. Seismic hazard curves for 5% damping at 0.0 (PGA), 0.05 and 0.1 s at INL and LANL.

Table A1
Mean annual frequencies of occurrence, $\Delta\lambda_i$, using PGA, 0.05 and 0.1 s hazard curves, annualized risk λ_{UP}[1], and percentage differences with respect to results calculated using 0.1 s hazard curves.

a. INL

i		$\Delta\lambda_i$			Difference[4], %	
		PGA	0.05 s	0.1 s	PGA	0.05 s
1		2.52×10^{-3}	2.22×10^{-3}	2.16×10^{-3}	17	3
2		1.57×10^{-4}	1.51×10^{-4}	1.54×10^{-4}	2	−2
3		3.53×10^{-5}	3.44×10^{-5}	3.53×10^{-5}	0	−3
4		1.15×10^{-5}	1.15×10^{-5}	1.19×10^{-5}	−3	−3
5		4.70×10^{-6}	4.60×10^{-6}	4.78×10^{-6}	−2	−4
6		1.99×10^{-6}	2.13×10^{-6}	2.32×10^{-6}	−14	−9
λ_{UP}	Simplified[2]	1.05×10^{-4}	9.94×10^{-5}	1.01×10^{-4}	4	−1
	Monte Carlo[3]	1.08×10^{-4}	1.02×10^{-4}	1.03×10^{-4}	5	−1

b. LANL

i		$\Delta\lambda_i$			Difference[4], %	
		PGA	0.05 s	0.1 s	PGA	0.05 s
1		8.31×10^{-4}	8.04×10^{-4}	7.94×10^{-4}	5	1
2		1.05×10^{-4}	1.04×10^{-4}	1.04×10^{-4}	0	0
3		3.64×10^{-5}	3.51×10^{-5}	3.50×10^{-5}	4	0
4		1.53×10^{-5}	1.47×10^{-5}	1.47×10^{-5}	4	0
5		6.87×10^{-6}	7.05×10^{-6}	7.21×10^{-6}	−5	−2
6		3.31×10^{-6}	3.68×10^{-6}	3.87×10^{-6}	−14	−5
λ_{UP}	Simplified[2]	7.17×10^{-5}	7.07×10^{-5}	7.09×10^{-5}	1	0
	Monte Carlo[3]	7.34×10^{-5}	7.24×10^{-5}	7.25×10^{-5}	1	0

[1] Mean annual frequency of unacceptable performance calculated per Eq. (7).
[2] Risk calculated using conditional failure probabilities in the fourth column of Table 5.
[3] Risk calculated using conditional failure probabilities in the fourth column of Table 6.
[4] Percentage difference in $\Delta\lambda_i$ or λ_{UP} with respect to those calculated using 0.1 s hazard curves.

References

American Society of Civil Engineers (ASCE), 2005. Seismic Design Criteria for Structures, Systems and Components in Nuclear Facilities. ASCE/SEI Standard 43-105, Reston, VA.

American Society of Civil Engineers (ASCE), 2010. Minimum Design Loads For Buildings and Other Structures. ASCE/SEI Standard 7-10, Reston, VA.

American Society of Civil Engineers (ASCE), 2017. Seismic Analysis of Safety-related Nuclear Structures And Commentary. ASCE/SEI Standard 4-16, Reston, VA.

Applied Technology Council (ATC), 2012. Seismic Performance Assessment of Buildings. Volume 1 – Methodology. FEMA P-58. Federal Emergency Management Agency, Washington, D.C.

Bolisetti, C., Whittaker, A.S., Mason, H.B., Almufti, I., Willford, M., 2014. Equivalent linear and nonlinear site response analysis for design and risk assessment of safety-related nuclear structures. Nucl. Eng. Des. 275, 107–121.

Bolisetti, C., Coleman, J.L., Talaat, M., Hashimoto, P., 2015. Advanced Seismic Fragility Modeling Using Nonlinear Soil-Structure Interaction Analysis. INL/EXT-15-36375. Idaho National Laboratory, Idaho Falls, ID.

Bolisetti, C., Yu, C.-C., Coleman, J., Kosbab, B., Whittaker, A.S., 2016. Characterizing the Benefits of Seismic Isolation to Nuclear Facilities: A Framework For Risk-Based Decisions Making. INL/EXT-16-40122. Idaho National Laboratory, Idaho Falls, ID.

Coleman, J.L., Bolisetti, C., Whittaker, A.S., 2015. Time-domain soil-structure interaction analysis of nuclear facilities. Nucl. Eng. Des. 298, 264–270.

Coleman, J.L., Bolisetti, C., Veeraraghavan, S., Parisi, C., Prescott, S.R., Gupta, A., Kammerer, A.M., 2016. Multi-hazard Advanced Seismic Probabilistic Risk Assessment Tools and Applications. INL/EXT-16-40055. Idaho National Laboratory, Idaho Falls, ID.

Constantinou, M.C., Whittaker, A.S., Kalpakidis, Y., Fenz, D.M., Warn, G.P., 2007. Performance of Seismic Isolation Hardware Under Service and Seismic Loading. MCEER-07-0012. University at Buffalo, The State University of New York, Buffalo, NY.

Dynamic Isolation System (DIS) Inc. Isolator engineering properties. < http://www.dis-inc.com/technical.html > (June 1, 2016).

Electric Power Research Institute (EPRI), 2013. Seismic Probabilistic Risk Assessment Implementation Guide. 3002000709, Palo Alto, CA.

Hancock, J., Watson-Lamprey, J., Abrahamson, N.A., Bommer, J.J., Markatis, A., McCoy, E., Mendis, R., 2006. An improved method of matching response spectra of recorded earthquake ground motion using wavelets. J. Earthquake Eng. 10 (spec01), 67–89.

Huang, Y.-N., Whittaker, A.S., Luco, N., 2008a. Performance Assessment of Conventional and Base-isolated Nuclear Power Plants for Earthquake and Blast Loadings. MCEER-08-0019. University at Buffalo, The State University of New York, Buffalo, NY.

Huang, Y.-N., Whittaker, A.S., Luco, N., 2008b. Maximum spectral demands in the near-fault region. Earthquake Spectra 24 (1), 319–341.

Huang, Y.-N., Whittaker, A.S., Luco, N., 2009a. Orientation of maximum spectral demand in the near-fault region. Earthquake Spectra 25 (3), 707–717.

Huang, Y.-N., Whittaker, A.S., Kennedy, R.P., Mayes, R.L., 2009b. Assessment of Base-isolated Nuclear Structures for Design and Beyond-design Basis Earthquake Shaking. MCEER-09-0008. University at Buffalo, The State University of New York, Buffalo, NY.

Huang, Y.-N., Whittaker, A.S., Luco, N., 2011a. A seismic risk assessment procedure for nuclear power plants, (I) methodology. Nucl. Eng. Des. 241, 3996–4003.

Huang, Y.-N., Whittaker, A.S., Luco, N., 2011b. A seismic risk assessment procedure for nuclear power plants, (II) application. Nucl. Eng. Des. 241, 4004–4011.

Kammerer, A., Whittaker, A.S., Constantinou, M.C. (forthcoming). Technical considerations for seismic isolation of nuclear facilities. NUREG-****, United States Nuclear Regulatory Commission, Washington, D.C.

Kumar, M., Whittaker, A.S., Constantinou, M.C., 2014. An advanced numerical model of elastomeric seismic isolation bearings. Earthquake Eng. Struct. Dynam. 43 (13), 1955–1974.

Kumar, M., Whittaker, A.S., Constantinou, M.C., 2015. Seismic Isolation of Nuclear Power Plants Using Sliding Bearings. MCEER-15-0006. University at Buffalo, The State University of New York, Buffalo, NY.

Kumar, M., Whittaker, A.S., Kennedy, R.P., Johnson, J.J., Kammerer, A.M., 2017. Seismic probabilistic risk assessment for isolated safety-related nuclear facilities. Nucl. Eng. Des. 313C, 386–400.

Livermore Software Technology Corporation (LSTC), 2013. LS-DYNA Keyword User's Manual – Version R 7.0. Livermore CA.

McVitty, W.J., Constantinou, M.C., 2015. Property Modification Factors for Seismic Isolators: Design Guidance For Buildings. MCEER-15-0005. University at Buffalo, The State University of New York, Buffalo, NY.

Pacific Earthquake Engineering Research (PEER), 2011. PEER ground motion database. < http://peer.berkeley.edu/peer_ground_motion_database > (June 1, 2016).

Reed, J.W., Kennedy, R.P., 1994. Methodology for Developing Seismic Fragilities. TR-103959. Electric Power Research Institute, Palo Alto, CA.

Stevenson, J.D., 1981. Evaluation of the Cost Effects on Nuclear Power Plant Construction Resulting From the Increase in Seismic Design Level. NUREG/CR-1508. United States Nuclear Regulatory Commission, Washington, D.C.

Stevenson, J.D., 2003. Historical development of the seismic requirements for construction of nuclear power plants in the U.S. and worldwide and their current impact on cost and safety. In: Transactions, 17th International Conference on Structural Mechanics in Reactor Technology (SMiRT-17), Prague, Czech Republic.

United States Geological Survey (USGS), 2008. 2008 Interactive deaggregations. < http://geohazards.usgs.gov/deaggint/2008/ > (June 1, 2016).

United States Geological Survey (USGS), 2012. Hazard curve application < https://geohazards.usgs.gov/hazardtool/application.php > (June 1, 2016).

Yang, T.Y., Moehle, J.P., Stojadinovic, B., Der Kiureghian, A., 2009. Performance evaluation of structural systems: theory and implementation. J. Struct. Eng. 135 (10), 1146–1154.